Magnetoencephalography contrast adaptation reflects perceptual adaptation

Erin Goddard
McGill Vision Research, Department of Ophthalmology & Visual Sciences, McGill University Montreal, Quebec, Canada
Present address: School of Psychology, UNSW, Sydney, Australia

Christopher Shooner
McGill Vision Research, Department of Ophthalmology & Visual Sciences, McGill University Montreal, Quebec, Canada

Kathy T. Mullen
McGill Vision Research, Department of Ophthalmology & Visual Sciences, McGill University Montreal, Quebec, Canada

Contrast adaptation is a fundamental visual process that has been extensively investigated and used to infer the selectivity of visual cortex. We recently reported an apparent disconnect between the effects of contrast adaptation on perception and functional magnetic resonance imaging BOLD response adaptation, in which adaptation between chromatic and achromatic stimuli measured psychophysically showed greater selectivity than adaptation measured using BOLD signals. Here we used magnetoencephalography (MEG) recordings of neural responses to the same chromatic and achromatic adaptation conditions to characterize the neural effects of contrast adaptation and to determine whether BOLD adaptation or MEG better reflect the measured perceptual effects. Participants viewed achromatic, L-M isolating, or S-cone isolating radial sinusoids before adaptation and after adaptation to each of the three contrast directions. We measured adaptation-related changes in the neural response to a range of stimulus contrast amplitudes using two measures of the MEG response: the overall response amplitude, and a novel time-resolved measure of the contrast response function, derived from a classification analysis combined with multidimensional scaling. Within-stimulus adaptation effects on the contrast response functions in each case showed a pattern of contrast-gain or a combination of contrast-gain and response-gain effects. Cross-stimulus adaptation conditions showed that adaptation effects were highly stimulus selective across early, ventral, and dorsal visual cortical areas, consistent with the perceptual effects.

Introduction

Adaptation to contrast has been extensively studied in vision and is believed to be part of a process of contrast normalization, in which the visual system shifts its dynamic range in response to the changing visual environment. Contrast adaptation is evident at many levels in the human visual system, including behavioral responses (Blakemore & Campbell, 1969; Blakemore & Nachmias, 1971; Gibson & Radner, 1937; Krauskopf, Williams, & Heeley, 1982; Krauskopf, Williams, Mandler, & Brown, 1986), cortical BOLD responses (Boynton & Finney, 2003; Engel, 2005; Engel & Furmanski, 2001; Fang, Murray, Kersten, & He, 2005; Gardner, Sun, Waggoner, Ueno, Tanaka, & Cheng, 2005; Grill-Spector & Malach, 2001; Krekelberg, Boynton, & van Wezel, 2006) and visual evoked potentials (VEPs) (Blakemore & Campbell, 1969; Campbell & Maffei, 1970; Dong, Du, & Bao, 2020; Duncan, Roth, Mizokami, McDermott, & Crognale, 2012). Electrophysiological recordings in non-human species have also characterized how contrast adaptation shifts the responses of single neurons (e.g., Movshon & Lennie, 1979); Ohzawa, Sclar, & Freeman, 1982; also see reviews by Kohn, 2007, and Solomon & Kohn, 2014).

For decades, adaptation has been widely used as a scientific tool to infer the tuning of distinct visual responses and has played an important role in defining selective responses for low level properties such as orientation, spatial frequency, and direction, as well as higher level visual responses (Webster,

Citation: Goddard, E., Shooner, C., & Mullen, K. T. (2022). Magnetoencephalography contrast adaptation reflects perceptual adaptation. *Journal of Vision*, *22*(10):16, 1–19, https://doi.org/10.1167/jov.22.10.16.

https://doi.org/10.1167/jov.22.10.16 Received January 20, 2022; published September 19, 2022 ISSN 1534-7362

2011; Webster, 2015). In color vision, behavioral adaptation experiments have inferred the presence of three distinct low-level responses (two cone opponent and one achromatic) (Krauskopf et al., 1982; Krauskopf et al., 1986). This, combined with other psychophysical approaches, allowed the definition of three cardinal stimuli, each of which selectively isolates one of the three postreceptoral responses. Subsequent measurements have shown that adaptation is not as cleanly selective as first thought (Webster & Mollon, 1994) and that the degree of selectivity depends on the type of behavior measured, whether detection thresholds or suprathreshold contrast appearance (Goddard, Chang, Hess, & Mullen, 2019). Hence, although a useful tool, adaptation in color vision is a complex process that is likely to involve many levels in the visual system.

Even with these caveats, it is important to know whether selective responses inferred by behavioral adaptation experiments are also evident using different measurement methods, such as single neuron recording or BOLD responses. These comparisons provide a means of identifying the physiological basis of behaviorally defined tuned responses, and also validating the assumptions made from the behavioral data. For example, given that color selectivity is found at a behavioral level, can we also expect to find selective responses at a physiological level? Mullen, Chang, & Hess (2015) and Goddard et al. (2019) directly tested the link between psychophysical and BOLD contrast adaptation with the overall aim of determining the cortical location of selectivity for color contrast. Although selective adaptation to color contrast was found psychophysically, the selectivity of BOLD responses measured under the same conditions was much weaker. Mullen et al. (2015) reported significant, but not complete, selective adaptation to stimuli isolating the L/M cone opponent responses, especially in the area VO of the ventral visual cortex. Some selectivity was also found for achromatic contrast in the dorsal cortical regions. Responses in other areas, including V1 and V2, were unselective, in contrast to previous reports of selectivity for L/M cone opponent and achromatic adaptation effects as early as V1 (Engel, 2005; Engel & Furmanski, 2001). Surprisingly, when the responses to S-cone isolating stimuli were included in a subsequent study (Goddard et al., 2019), no selectivity was found in any cortical area tested. Instead, there was a strong cross-stimulus adaptation between S-cone isolating and achromatic contrast that matched the within-stimulus adaptation both for S-cone isolating and achromatic test stimuli. This disconnect in the selectivity of adaptation to color contrast for BOLD compared with behavior is one example of a remaining gap in our understanding of contrast adaptation.

Here, we aim to better understand the neural processes underlying contrast adaptation in human visual cortex using a complementary measure of neural activity. We use magnetoencephalography (MEG) measurements in a comparable study of cross- and within-stimulus adaptation as we have used previously both psychophysically and for BOLD (Goddard et al., 2019; Mullen et al., 2015). Unlike BOLD measurements, MEG measures signals related to the electrical activity of neurons independently of blood oxygenation levels. In this way, MEG is similar to VEP measurements, which have previously been used to measure chromatic adaptation (Rabin, Switkes, Crognale, Schneck, & Adams, 1994), chromatic contrast adaptation within the isoluminant plane (Duncan et al., 2012), and achromatic contrast adaptation (e.g., Blakemore & Campbell, 1969; Dong et al., 2020). Unlike these VEP studies, which were focused on responses the occipital pole, here we use MEG to simultaneously measure from multiple sites across the cortex, including signals from ventral visual areas (e.g., as in Bartsch, Loewe, Merkel, Heinze, Schoenfeld, Tsotsos, & Hopf, 2017), which are particularly relevant here since area VO was a site of selective adaptation in the previous BOLD adaptation work whereas V1 was not (Mullen et al., 2015). MEG has been used to measure reliably different patterns of cortical response to isoluminant stimuli varying only in chromaticity (e.g., Rosenthal, Singh, Hermann, Pantazis, & Conway, 2021; Teichmann, Grootswagers, Carlson, & Rich, 2019; Teichmann, Quek, Robinson, Grootswagers, Carlson, & Rich, 2020).

Using MEG, we measured within- and cross-stimulus adaptation for the same chromatic and achromatic stimuli as used in previous work. We report the effects of adaptation on the overall amplitude of visual cortical responses to stimuli across a range of contrast levels, and we introduce a new analysis of contrast response functions based on multivariate classification analyses in conjunction with multidimensional scaling. We find strong evidence of selective adaptation across all visual areas, consistent with the behavioral effects of these stimuli.

Materials and methods

Participants

We collected MEG data on six participants (four female, two male, aged 22-35 years). Five of the six participants participated in the psychophysical experiments reported in our previous work (Goddard et al., 2019), and their data are included in the replotted psychophysical data in Figure 7. In addition, three of the six current participants who participated in one or more of the functional magnetic resonance imaging (fMRI) adaptation experiments in our previous work (Goddard et al., 2019; Mullen et al., 2015).

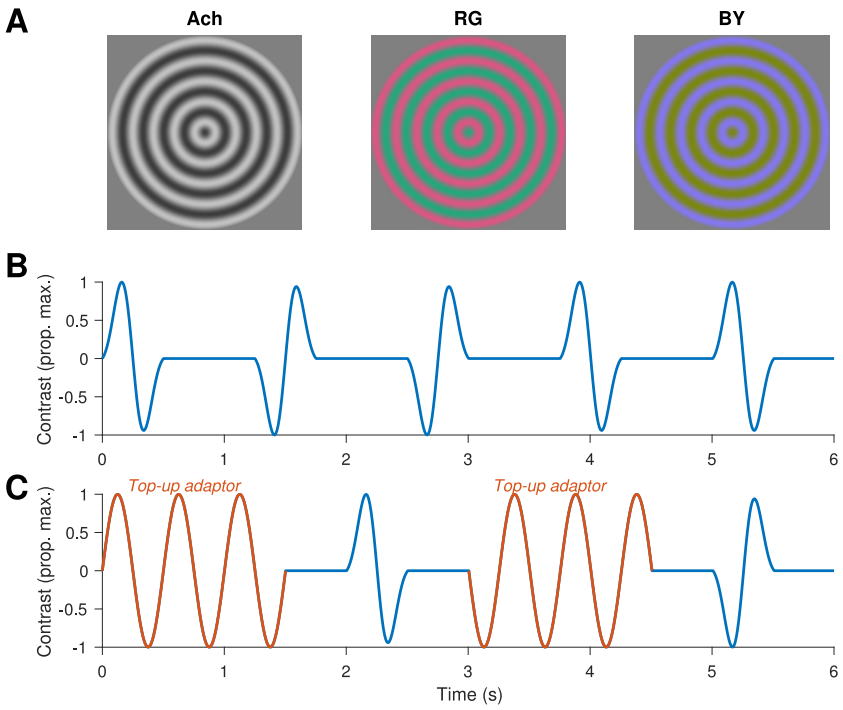

Figure 1. Spatial and temporal stimulus properties. (A) Adaptor and test stimuli were radial sinewave gratings calibrated to isolate the Ach, RG, or BY responses. (B) Example time course of "no adaptor" blocks with test stimulus trials shown in blue, each including one cycle of the 2 Hz sinusoidal contrast phase alternation in the 500 ms test interval. (C) Example time course of "adapt" blocks, with 1.5 seconds of top-up adaptor shown in *orange* (that follows a single 60-second initial adaptation), and test stimulus trials shown in *blue*. In one MEG recording session, one type of adaptor was shown (Ach, RG, or BY) but across trials test stimuli were either Ach, RG, or BY.

Participants who participated in the MEG experiment reported here each completed an MRI session in which we acquired high-resolution anatomical images of their brains and functional data used to define regions of interest. All participants were healthy with no history of neurological or psychiatric disorders and provided informed consent. Each participant had normal or corrected-to-normal visual acuity, and normal color vision as assessed with Ishihara plates (Ishihara, 1990) and the Farnsworth-Munsell 100-hue test (Farnsworth, 1957). All experimental procedures were approved by the Ethics Review Board of the McGill University Health Centre and were conducted in accordance with the Declaration of Helsinki.

Visual stimuli

All stimuli in the MEG experiment were radial sinewave gratings, as used in previous work (Goddard et al., 2019; Goddard & Mullen, 2020; Mullen, Dumoulin, McMahon, de Zubicaray, & Hess, 2007; Mullen et al., 2015). For each of the three stimulus types, contrast was either achromatic (Ach), isoluminant "red-green" (RG), or "blue-yellow" (BY), modulated about a mean gray, and calibrated to isolate the luminance, L/M cone opponent, or S-cone opponent responses, respectively. The stimuli each had a spatial frequency of 0.5 cycles/deg, and a 2 Hz sinusoidal contrast phase alternation. The low spatial frequency of the two chromatic stimuli reduces luminance artifacts generated by chromatic aberration for the chromatic stimuli (Bradley, Zhang, & Thibos, 1992; Cottaris, 2003; Mullen, 1985). Each radial sinewave grating was 19° in diameter and outside the stimulus area the screen was at its mean luminance, as illustrated in Figure 1.

Stimulus chromaticity was defined in a three-dimensional cone contrast space, with each axis representing the quantal catch of the L, M and S cone types normalized with respect to the grey background (i.e., cone contrast). The vector direction and length within this space defines chromaticity and cone contrast respectively. We note that this definition differs from Michelson contrast because a full-contrast achromatic grating modulates each cone by 100% (LMS = [1,1,1]) and so has a total cone contrast of $\sqrt{3}$ (173%). We determined isoluminance of the RG stimuli for each subject individually based on perceptual minimum motion settings as previously described (Mullen, Thompson, & Hess, 2007; Mullen et al., 2010). Each participant adjusted the proportion of RG color to luminance contrast in a downward drifting grating until its perceived motion/flicker was at a minimum. The grating was 0.5 cycle/deg, 10° diameter, with 5Hz drift,

and the isoluminance settings were repeated at least 5 times then averaged for each participant. We used the standard S-cone isolating direction for all observers. We verified that this direction was the optimal for isolation of the S-cones for each participant by using a method or adjustment to varying vector angle within the isoluminant plane to determine the direction of minimum visibility (Michna, Yoshizawa, & Mullen, 2007). In all subjects, this corresponded closely to the S-cone isolating axis.

For adapting stimuli, we chose high stimulus cone contrasts (48% for Ach, 9.3% for RG, and 40% for BY), with the aim of inducing robust adaptation effects. For each test stimulus type, we used a range of 4 logarithmically spaced stimulus cone contrasts (Ach: 18%–123%, RG: 1.4%–14%, and BY: 7.1%–57%), in each case including contrasts that were highly visible to maximize the chance of evoking visual responses that would be measurable with MEG. The three types of stimuli were chosen to be at the upper end of the available contrast range to maximize the adaptation effects. Contrasts are higher than those used in our previous publications (e.g., Goddard et al., 2019; Mullen et al., 2007) because the ProPixx DLP LED projector used here was capable of generating higher color contrasts. The cone contrast levels are different across Ach, RG and BY stimuli as the visual system has differing levels of sensitivity to these three different contrast types (Sankeralli & Mullen, 1996). Approximately, our contrasts are 30 times threshold for the two chromatic stimuli and 40 times threshold for the achromatic stimulus.

MEG methods: Acquisition protocols

MEG data were collected with a whole-head MEG system (CTF OMEGA System) consisting of 275 axial gradiometers. For each MEG session we first collected five minutes of empty room recordings, which we used to estimate noise covariance of the sensors (see below). Before the participant entering the magnetically shielded room, three marker coils were placed on the participant's head. Marker positions, nasion, left and right pre-auricular points, and the participant's head shape were recorded with a pen digitizer (Isotrak; Polhemus, Colchester, VT, USA), using a minimum of 500 points. Two electrooculogram electrodes were places above and below the left eye, to record eye blinks and eye movements during the MEG session. Two electrodes were placed across the plane of the chest to collect electrocardiographic signals, and a reference electrode was placed below the participant's collarbone. Each participant's MEG data and simultaneous electrooculographic and electrocardiographic signals were collected at a sampling frequency of 2400Hz. In conjunction with these data, we collected participants' button responses using a Vpixx ResponsePixx button box system (VPixx Technologies, Saint-Bruno-de-Montarville, QC, Canada).

MEG methods: Display apparatus and calibrations

We displayed stimuli using a PROPixx DLP LED projector (VPixx Technologies; resolution 1920 × 1080), located outside the magnetically shielded room, to back-project images onto a custom screen via two mirrors. Participants, lying supine in the MEG system, viewed the custom screen, located above them, from a distance of 45 cm. We used a Windows PC (Windows 7) running MATLAB (R2017a; MathWorks, Inc., Natick, MA, USA) in conjunction with routines from Psychtoolbox 3.0 (Brainard, 1997; Kleiner, Brainard, & Pelli, 2007; Pelli, 1997) to generate and project the stimuli (refresh rate 60Hz, mean luminance 106 cd/m^2). The PROPixx DLP LED projector has a linear gamma, and was color calibrated as described previously (Michna et al., 2007; Mullen et al., 2007; Mullen, Dumoulin, & Hess, 2008). We precisely aligned stimulus presentation times with the recorded MEG data using the VPixx "Pixel Mode" to record the output of a single pixel along with the MEG data.

MEG methods: Experimental design and participant's task

Each participant completed three MEG sessions on different days, each separated by at least one week. All test stimuli were used in all sessions. Across different sessions the participants were adapted to either the Ach, RG or BY adaptor stimulus: each session included a single adaptor stimulus, and the order of these was counterbalanced across participants. Each MEG session was divided into six blocks of eight to nine minutes each, with breaks between blocks.

A total of 694 trials without any adaptation were split across the first two blocks of each session, followed by another 694 trials with adaptation, which were split across the remaining four blocks. Across trials, test stimuli were either Ach, RG, or BY contrast, at one of four contrast levels. Each test stimulus was 500 ms, including one full cycle of the 2 Hz sinusoidal modulation. The 500 ms sinusoidal modulation was presented within a temporal Gaussian envelope (sigma 125 ms), resulting in a contrast modulation with the temporal profile plotted in Figure 1. Contrast polarity was reversed on half the trials, giving a total of 24 unique test stimuli (3 types × 4 contrasts × 2 polarities), to which we added a blank trial type of the mean grey screen. Participants viewed each stimulus trial type 26 times, and the blank trial type 52 times, giving the total 694 trials in each no-adapt and adaptation condition.

These 694 trials were counterbalanced so that each trial type was equally likely to be preceded by every other trial type.

In the no-adaptation conditions, the 500 ms stimuli were presented with 750 ms intertrial intervals of a mean gray blank screen, as shown in Figure 1B. The first adaptation block commenced with 60 seconds' initial adaptation, whereas the remaining adaptation blocks commenced with 15 seconds' initial adaptation. Each trial during the adaptation conditions commenced with 1.5-second top-up adaptation, followed by 500 ms blank screen, before the 500 ms test stimulus, and then a 500 ms intertrial interval, as shown in Figure 1C. Initial and top-up adapting stimuli all modulated at 2 Hz, starting from zero contrast and including a whole number of cycles so that the 2 Hz modulation also terminated at zero contrast.

A small circular fixation marker was displayed in the center of both adapting and test stimuli (dot diameter 0.1°). This fixation dot was usually dark gray (a 40% decrement from the background), but to ensure they were fixating, participants were required to respond with a button press whenever they saw the fixation dot change to darker (80% decrement) or lighter (20% increment). These changes were always transient (200 ms duration) and occurred during a quarter of the trials (randomly selected). The exact onset of the increment or decrement varied randomly within the trial, but during the adaptation conditions the fixation change always occurred during the adaptor period of the trial. For the no-adaptation conditions, trials including a fixation change were repeated, and data from trials where a fixation change occurred were discarded from the analysis. We evaluated participants' performance on this task using their hit rate (HR; proportion of fixation-change present trials with a button press) and false alarm rate (FA; proportion of fixation-change absent trials with a button press) to calculate sensitivity (d′) using the MATLAB function *norminv* (inverse of the cumulative normal distribution), where

$$d' = norminv\,(\mathrm{HR}) - norminv\,(\mathrm{FA})$$

Across participants, the average d′ was 0.97 (standard error 0.15).

MRI methods: Retinotopic and functional localizers

All magnetic resonance imaging took place at the McConnell Brain Imaging Centre, McGill University, Montreal, Canada. For each participant we acquired two high-resolution three-dimensional whole head T1 images using an MP-RAGE sequence (TI = 900 ms, TR = 2300 ms, TE = 3.41 ms, 1.0 mm^3 resolution), and averaged these two images to generate the participant's anatomical template. Functional T2* MR images were acquired on a 3T Siemens MAGNETOM Prisma system (Siemens Medical Solutions, Malvern, PA, USA) with 32-channel head coil. Gradient-echo pulse sequences were used to measure blood oxygenation level-dependent (BOLD) signal as a function of time. We identified the visual cortical regions V1, V2, V3, V3A/B, LO1/LO2 and hV4 for each participant using rotating wedge stimuli and expanding and contracting concentric rings (Engel, Rumelhart, Wandell, Lee, Glover, Chichilnisky, & Shadlen, 1994; Sereno, Dale, Reppas, Kwong, Belliveau, Brady, Rosen, & Tootell, 1995), standard definitions of these areas (Brewer, Liu, Wade, & Wandell, 2005; Goddard et al., 2011; Larsson & Heeger, 2006), and the foveal confluence (Schira, Tyler, Breakspear, & Spehar, 2009). To localize areas VO1, VO2, and hMT+ we used data from the retinotopic mapping scans in conjunction with functional localizers for VO (Mullen et al., 2007) and hMT+ (Huk, Dougherty, & Heeger, 2002). Full details of our retinotopic mapping procedures, including scanning protocols, data preprocessing and area definition have been described previously (Goddard et al., 2019).

MEG data analysis: Preprocessing and source reconstruction

Preprocessing, forward modeling and source reconstruction of MEG data were performed using Brainstorm (Tadel, Baillet, Mosher, Pantazis, & Leahy, 2011, http://neuroimage.usc.edu/brainstorm). For each participant's template anatomical (a high-resolution MRI image), we used the automatic segmentation processes from Freesurfer 6.0 (Dale, Fischl, & Sereno, 1999; Fischl, Sereno, & Dale, 1999) to define the gray/white matter and pial/gray matter boundaries. Using Brainstorm, we imported the output of Freesurfer and created a 15,000-vertex model of each participant's cortical surface. For each block of trials in the MEG data, we aligned the participant's cortical surface model to the median measured marker coil locations for that block by aligning the head shape data from the MRI with the head shape relative to the marker coils, as recorded with the pen digitizer. For each functional run, we generated a forward model for each model by applying a multiple spheres model (Huang, Mosher, & Leahy, 1999) to the participant's cortical surface model at this measured head location.

Functional data were preprocessed in Brainstorm with notch filtering (60, 120, and 180 Hz), followed by bandpass filtering (0.2–200 Hz, using the Brainstorm default of an even-order linear phase finite impulse response filter). We preprocessed data from the empty

room recording using identical protocols, then used the output to estimate the noise covariance for the session. Cardiac and eye blink artifacts were removed from functional data using signal space projection: cardiac and eye blinks events were identified using default filters in Brainstorm, manually verified, then used to estimate a small number of basic functions corresponding to these noise components, which were removed from the recordings (Uusitalo & Ilmoniemi, 1997). From these functional data we extracted an epoch of data for each trial: from −100 to 1000 ms relative to stimulus onset, and down-sampled to 100 Hz. Using the noise covariance estimate, regularized using the median eigenvalue, we applied a minimum norm source reconstruction to this trial data.

For classification analyses we generated three datasets using each participant's functionally defined cortical areas. In the "early visual cortex" (EVC) region of interest, we included data from all vertices located within areas V1, V2 and V3, while the "ventral visual cortex" (VVC) region of interest included areas hV4, VO1 and VO2, and "dorsolateral visual cortex" (DVC) included areas V3A/B, LO1, LO2 and hMT+. We found very similar adaptation effects across these Regions of Interest (ROIs), which we believe most likely reflects the failure of the source reconstruction to completely isolate responses from these adjoining cortical regions, although it is possible that the adaptation effects reported below are genuinely very similar across these cortical areas. Because there is little difference across ROIs, in most cases below we show data from EVC only, but equivalent figures for VVC and DVC are included in Supplementary Material.

MEG data analysis: Contrast response functions estimated from response amplitude

We measured the amplitude of stimulus-evoked responses from the MEG data for each stimulus type (each color, at each contrast), from each session, both before and after adaptation. For each trial's evoked response, we averaged across source locations and subtracted the average activity across all blank trials (from the same session and adaptation condition), before taking the root mean square across trials to obtain a measure of the average evoked response. Examples of these measures are shown in Figure 2.

To reduce these average timecourses to a single measure of response amplitude, we fit a simple model of the stimulus response from 50 to 600 ms after stimulus onset as the sum of two gamma probability density functions ($f(t)$), with shape and rate parameters α and β, given by:

$$f(t;\alpha,\beta) = \frac{\beta^{\alpha} t^{\alpha-1} e^{-\beta t}}{\Gamma(\alpha)}$$

In total, the model had seven free parameters: the delay, dispersion, and scaling (maximum) of the first and second peaks (three parameters per peak), and a response offset added to every time point. We used this simple double-peaked model to capture the shape of the responses to the counter-phasing stimuli, where each stimulus trial included one cycle (as shown in Figure 1). For each participant, we fit this model separately to the average root mean square response to every stimulus contrast in each adaptation condition, including separate no-adapt conditions for each adaptor, to ensure we were always comparing adapted and unadapted responses that were collected during the same session. From the model fits we obtained an overall measure of response amplitude in each case using the maximum minus minimum fitted value. We also fit the model to each blank trial condition to obtain a baseline measure (an estimate of response amplitude when the model is fit to non-stimulus-related fluctuations), which we subtracted from trial response amplitudes.

MEG data analysis: Contrast response functions estimated from classification-based analyses

In addition to the response amplitude estimates, we also used classification analyses in combination with multidimensional scaling (MDS) as an alternative measure of contrast response responses. We repeated the analysis for each 10 ms bin to capture how trial responses changed over time. For each data set (data from a single ROI from a single participant), we reduced the data using Principal Component Analysis (PCA), then used this reduced data in the classification analyses. Out of the total 15,000 sources in each participant's head model, the EVC ROI included an average of 725 sources (standard deviation [SD] = 177), the VVC ROI included an average of 390 sources (SD = 74), and the DVC ROI included an average of 449 sources (SD = 110). We reduced these with PCA and retained data from the first n components, which accounted for 99.9% of the variance, for the classification analysis (mean = 31.5, SD = 4.9 for EVC; mean = 29.8, SD = 5.4 for VVC; mean = 41.3, SD = 6.5 for DVC).

Within each of nine combinations of stimulus (Ach, RG, and BY) and adaptor type (Ach, RG, and BY) we conducted a series of pairwise classifications. We trained classifiers to discriminate each pair of unique trial types (2 phases × 5 contrast levels, including blank trials × 2 adaptation states = 20 trial types). In each case, we trained classifiers to discriminate between two categories of trial and tested on held-out data. We report results obtained with a linear support vector machine (SVM) classifier, using the MATLAB function *fitcsvm* with "*KernelFunction*" set to *"linear."* For all analyses we expressed average classifier accuracy in d' (a

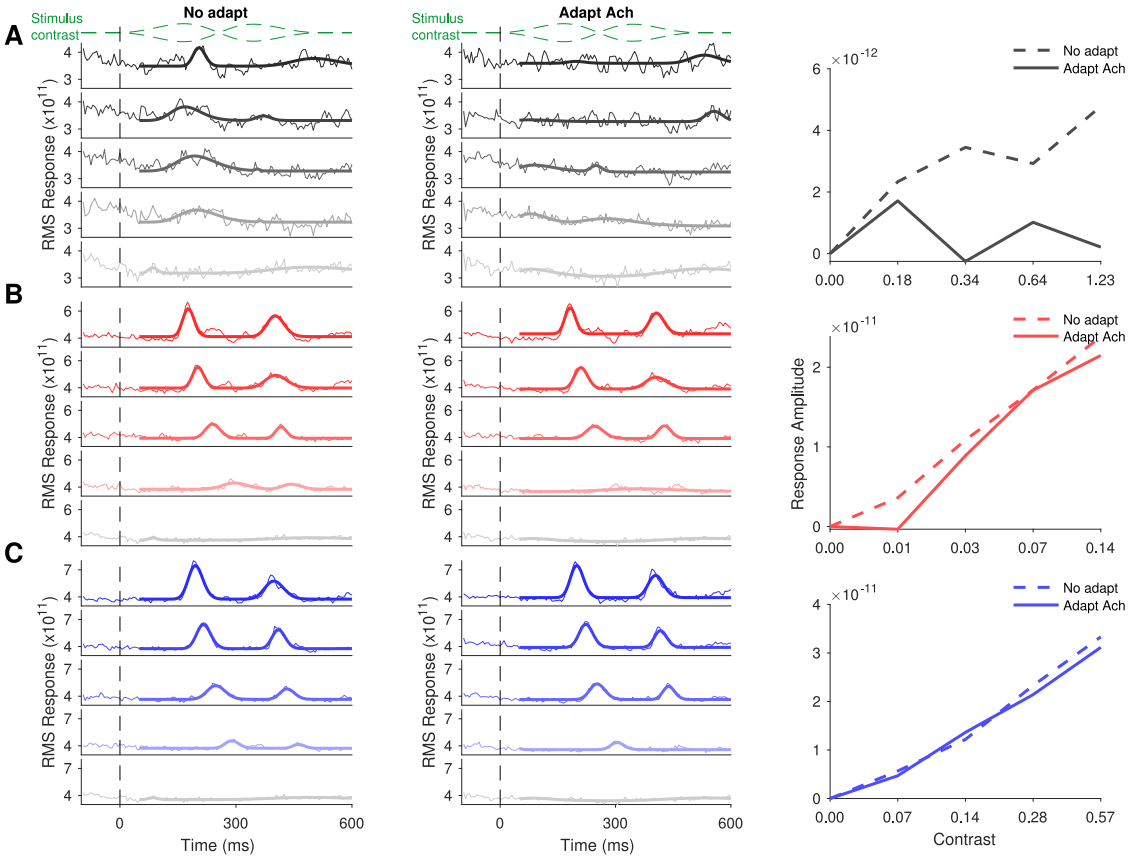

Figure 2. Example data for one participant under one adaptation condition (adapt Achromatic). The leftmost and center columns have the same plotting conventions and show data following no adaptor and an achromatic adaptor respectively, with the stimulus contrast over the same timescale shown in dashed green lines of the uppermost plot (the two lines show the two stimulus phases). In the remaining plots of the leftmost and center columns, responses to each test stimulus (A, achromatic; B, RG; C, BY) are plotted at each contrast (four contrasts in descending order from upper to lower plots, with response during blank trials in lowermost plots). *Thin lines* give average responses and thicker lines give best-fitting model response to the same data. The model was the sum of two gamma functions to capture the two-peaked responses to the counter-phasing stimuli (each trial included one full cycle). Model fits to blank trials were included to estimate baseline response. Raw data are shown from −100 to 600 ms relative to stimulus onset, but only data from 50 to 600 ms after stim onset were fit with the model. From these model fits, we summarized response amplitude at each contrast using the maximum minus minimum, minus the same measure for baseline (blank trials). Response amplitudes for this subject/adaptation condition are shown in the rightmost plots.

unit-free measure of sensitivity). Chance classification performance yields $d' = 0$.

These pairwise comparisons resulted in a dissimilarity matrix for each time bin (as illustrated in Figure 4), where each cell of the matrix was defined by classifier accuracy. We used the pattern of classifier accuracy across all 20 trial types to estimate contrast response. Reasoning that variation in responses to these trial types should be well captured by a single dimension of variation (corresponding to contrast response), we used multidimensional scaling (MDS) to reduce each dissimilarity matrix to a distribution of 20 values along a single dimension. Each MDS was completed using the MATLAB function *mdscale* with "*criterion*" set to *"metricstress"* (minimizing the stress normalized with the sum of squares of the dissimilarities). From the MDS solution, we used the distance of trial type from the average of the blank trial types as an alternate measure of response amplitude, in this way constructing contrast response functions for individual 10ms time bins. An example pair of contrast response functions generated by this process (for adapt Ach and no adapt trials) is shown in Figure 4. To investigate the effect of adaptation on the shape of the contrast response functions, we fit each contrast response function (obtained from the MDS solution) using a Naka-Rushton equation (as implemented by the *Psychtoolbox* function *ComputeNakaRushton*, with three input variables).

Statistical analyses

From the response amplitude estimates described above we obtained a single measure of the contrast response function for each stimulus color under each

adaptation condition. From the classification-based analyses, we obtained similar contrast response functions, but with finer temporal resolution, because we performed the analysis within each 10 ms time bin. In both cases we summed the responses across the four non-zero contrasts to obtain a single measure of response amplitude, equivalent to the area under the curve of the relevant contrast response function. To estimate the effect of each adaptor on each test stimulus, we compared the stimulus responses with and without adaptation.

We tested the statistical significance of each adaptation effect using a series of one-sided t-tests ($df = 5$). For each test stimulus, we also used a series of one-sided paired t-tests ($df = 5$) to test whether within-stimulus exceeded cross-stimulus adaptation for the remaining stimulus colors. For all t-tests we corrected for multiple comparisons using a false discovery rate (FDR) correction of $q < 0.05$ (Benjamini & Hochberg, 1995). We also used a Bayes factor analysis, an alternative to the traditional frequentist approach (Kass & Raftery, 1995; Morey & Wagenmakers, 2014). A Bayes factor compares evidence for competing hypotheses; here we report where there is moderate (BF > 3) or strong (BF > 10) evidence in favor of the alternate hypothesis, or at least moderate (BF < 1/3) evidence in favor of the null hypothesis. We implemented all Bayes Factor analyses using a MATLAB package (Krekelberg, 2021).

Results

We used MEG to measure the effects of within- and cross-stimulus contrast adaptation on neural responses to radial sinusoidal gratings of achromatic (Ach), L-M (RG) or S-cone isolating (BY) contrast, and we have analyzed the data using both changes in response amplitude and a classification method in conjunction with MDS.

Response amplitude analysis

In this section, we report the effects of contrast adaptation on response amplitude, averaged across early visual cortex. We estimate response amplitude using a simple model fit, as illustrated for an example participant and adaptor condition in Figure 2.

Average contrast response functions, across all participants and for each stimulus condition, are shown in Figure 3 (equivalent figures with data from

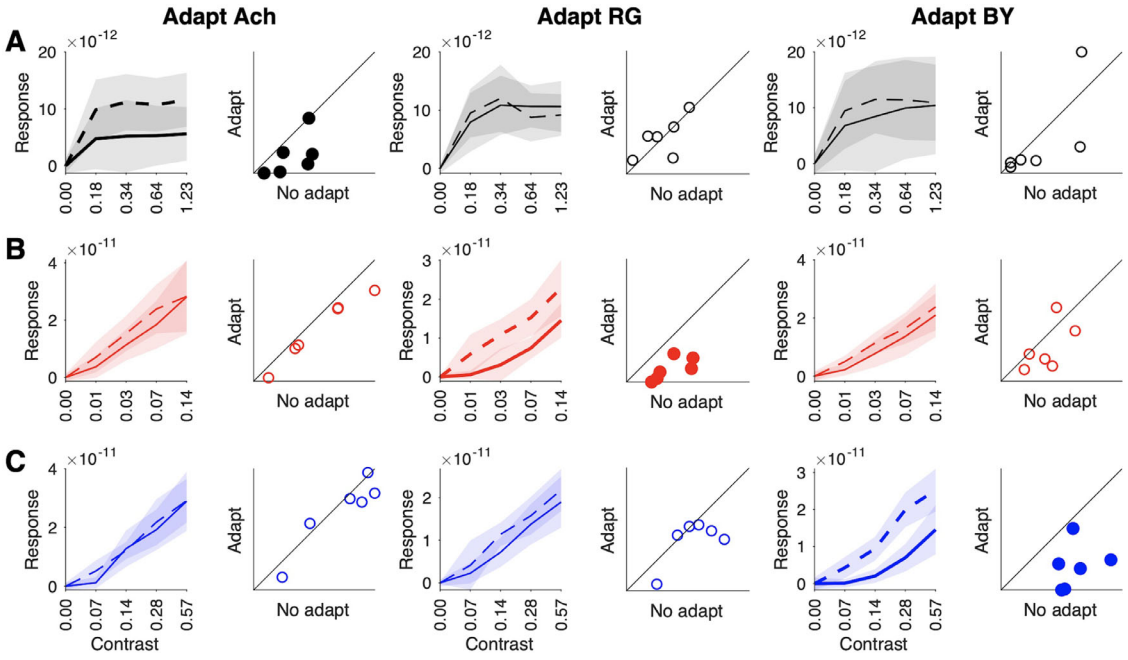

Figure 3. Effect of adaptation on average response across all adaptation conditions. Each pair of plots (line plot and scatterplot) show data for a single test stimulus (A, Ach; B, RG; C, BY) and a single adaptation condition (see titles at the top of each column). Line plots follow the conventions of those in the rightmost plots of Figure 2. The shaded regions give 95% confidence intervals of the between-subject mean (n = 6). The scatter plots show the same data condensed to an area under the curve (i.e., the sum of the responses at each non-zero stimulus contrast) for the no adapt condition (x-axis) versus for the adapt condition (y-axis). In the scatter plots, each marker shows data for a single subject. Results of statistical analyses of these adaptation effects are shown in Figure 7C, where data from the scatter plots are replotted. Cases of within-stimulus adaptation are highlighted with *bold lines* (line plots) and *filled markers* (scatterplots).

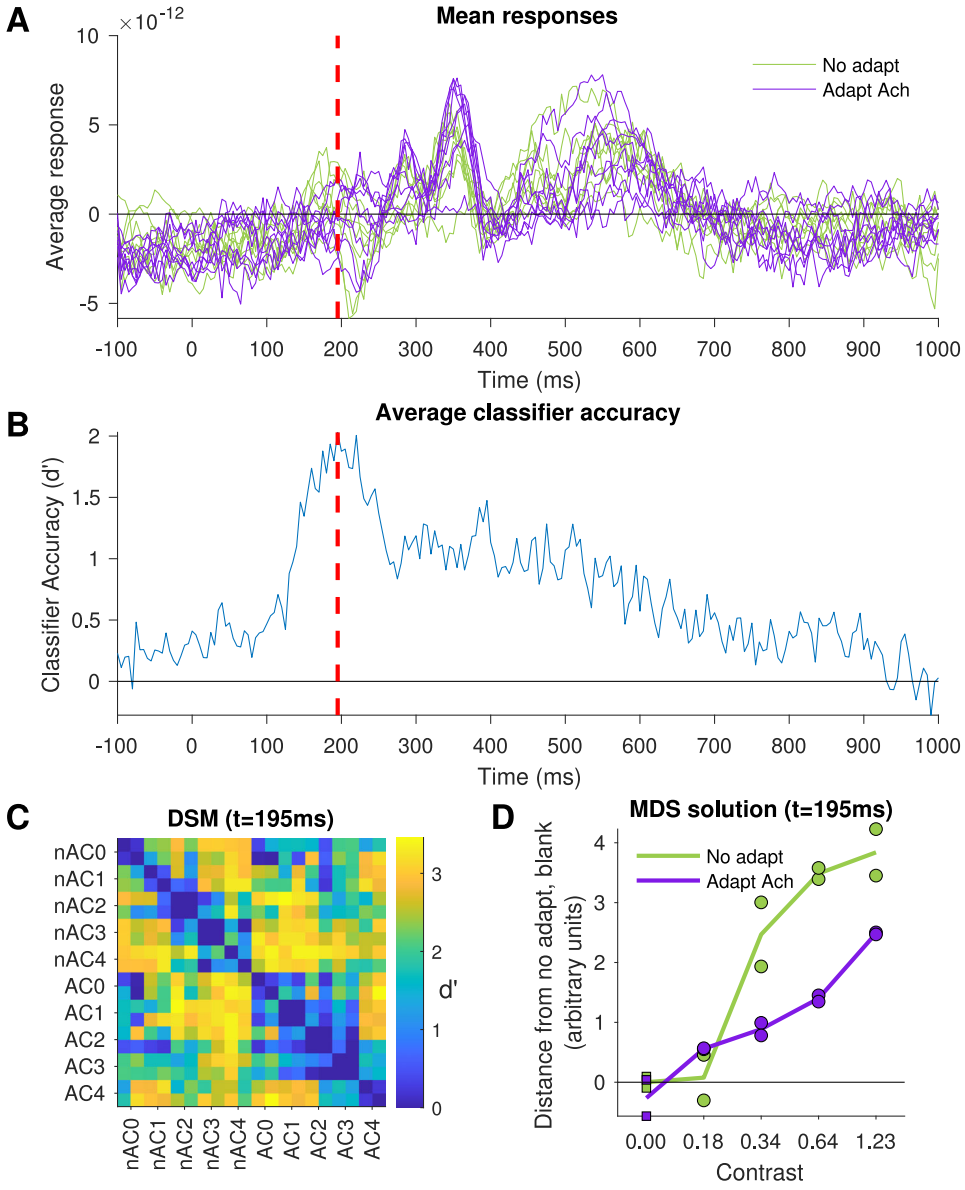

Figure 4. Illustration of classification and MDS-based approach for an example participant, in one condition (achromatic test stimulus, during the achromatic adaptation session): the same data as shown in Figure 2. (A) Average response to the 20 unique achromatic or blank trial types during this session, with line colored according to whether or not they were presented during adaptation. (B) Average classifier performance for pairwise discriminations of each of the 20 trial types. (C) Dissimilarity matrix (DSM) for a single time bin (t = 195 ms, maximum classifier performance, highlighted with *red dashed lines* in A and B). Trial types are labeled according to adaptation condition and contrast level (nA/A = no adapt/adapt, C0 = blank, C4 = max contrast), each label includes two rows/columns of the same contrast/adapt condition but different phases. (D) Contrast response functions obtained from MDS (applied to the DSM in C). Each circle corresponds to a response to an Ach stimulus of contrast given by the x-axis (square icons are blank trials: average location was used to define the zero response). Lines show the averages of the two phases of each trial type (circles of same color at each contrast). For the blank trials the two phases were identical.

ventral and dorsal visual cortex are shown in the Supplementary Material). For all stimuli (Ach, RG and BY), we found evidence of within-stimulus adaptation, but weak or no evidence of cross-stimulus adaptation. Across conditions, responses to Ach stimuli showed more evidence of saturating within the range of stimulus contrasts, whereas responses to RG and BY stimuli increased with contrast across the entire range of stimulus contrasts.

Classification analysis

As an alternative analysis, which did not rely on fitting response curves across the entire duration of

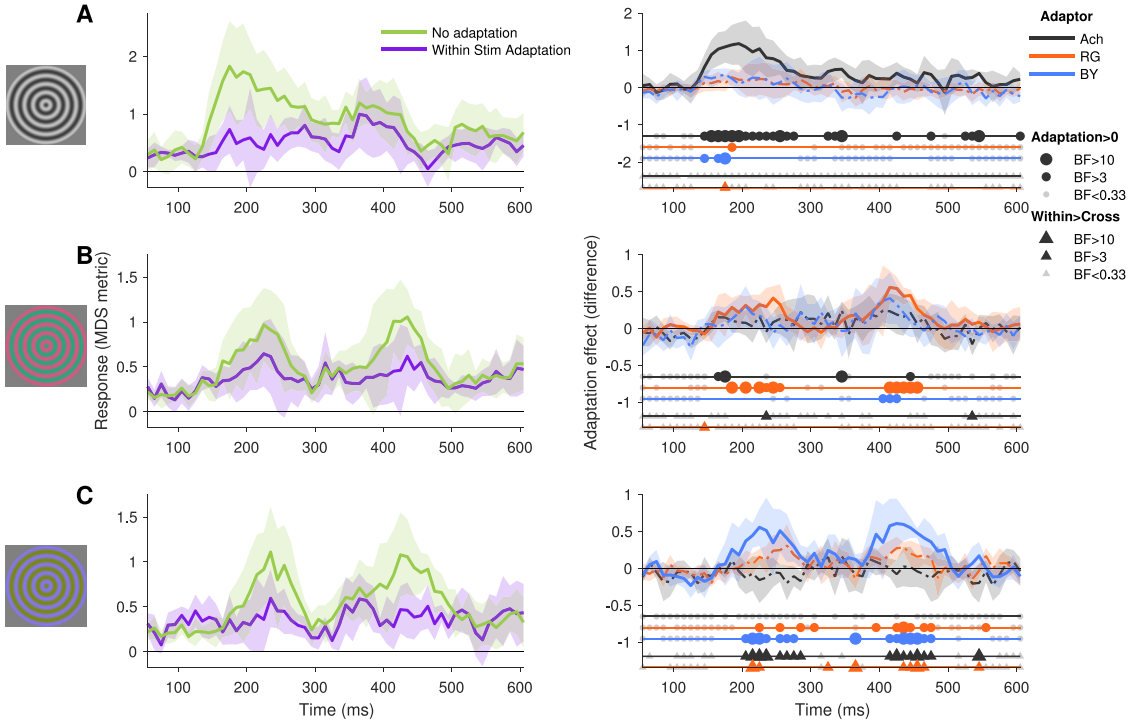

Figure 5. Effect of adaptation on overall level of response to Ach (A), RG (B) and BY (C) stimuli over time, as measured using area under the MDS-based contrast response functions. Left plots show stimulus response during no-adapt and within-stimulus adaptation. Right plots show the difference (Adapted response minus unadapted response) for both within-stimulus (*filled lines*) and cross-stimulus (*dashed lines*) adaptation. *Shaded regions* indicate the 95% confidence intervals of the between-subjects mean. Below the data in the right plots, results of the Bayes factor analysis, applied to data from each 10 ms bin, are shown. *Colored circles* show times where that adaptor reduced the response to the test stimulus, whereas *colored triangles* show times where that cross-stimulus adaptor induced a smaller effect than the within-stimulus adaptor. For both *circles* and *triangle*, small gray markers show times where there was at least moderate evidence (BF $<$ 0.33) in favor of no effect.

the stimulus-induced response, we used classification methods in conjunction with MDS to obtain a measure of contrast response function for each 10 ms time bin, as described in the Methods above and illustrated in Figure 4. Because this method is sensitive to stimulus-related information carried by the pattern of information across a region of interest (here, early visual cortex), it potentially detects subtler differences in the neural responses across stimulus contrast that may not be present in the overall amplitude of the response, or its variability across trial-types. This is illustrated in Figure 4, where greater variation in average responses to trials of different types (Figure 4A) does not predict times of greatest classifier performance (Figure 4B).

This analysis yielded estimates of contrast response functions for each time bin. We used these to consider two aspects of the effects of contrast adaptation on the responses to these stimuli: the effect of adaptation across the timecourse of the stimulus-induced response, and the effect of each adaptation condition on the shape of the contrast response function.

The effect of adaptation across the timecourse of the stimulus-induced response is shown in Figure 5 (equivalent figures with data from ventral and dorsal visual cortex are shown in the Supplementary Material). Consistent with the effects of adaptation on response amplitude (Figure 3), here we found that within-stimulus adaptation tended to be greater than cross-stimulus adaptation across all stimulus types. For BY stimulus responses, the effects of adaptation were consistent across both peaks of the response to the counter-phasing stimulus, and both peaks included time bins where there were strong effects (BF $>$ 10) of within-stimulus adaptation exceeding cross-stimulus adaptation. For RG stimulus responses, there were again within-stimulus adaptation effects at both peaks, but weaker evidence from the Bayes Factor analysis that these exceeded cross-stimulus adaptation. For the Ach stimulus, there was stronger within-stimulus adaptation around the first peak compared with the second peak of the response, but this was primarily driven by a larger response to the first peak than the second in the no adaptation condition, rather than a stronger response to the second peak in the adapted condition. The response to the Ach stimulus showed robust within-stimulus adaptation effects, but weak evidence that this within-stimulus

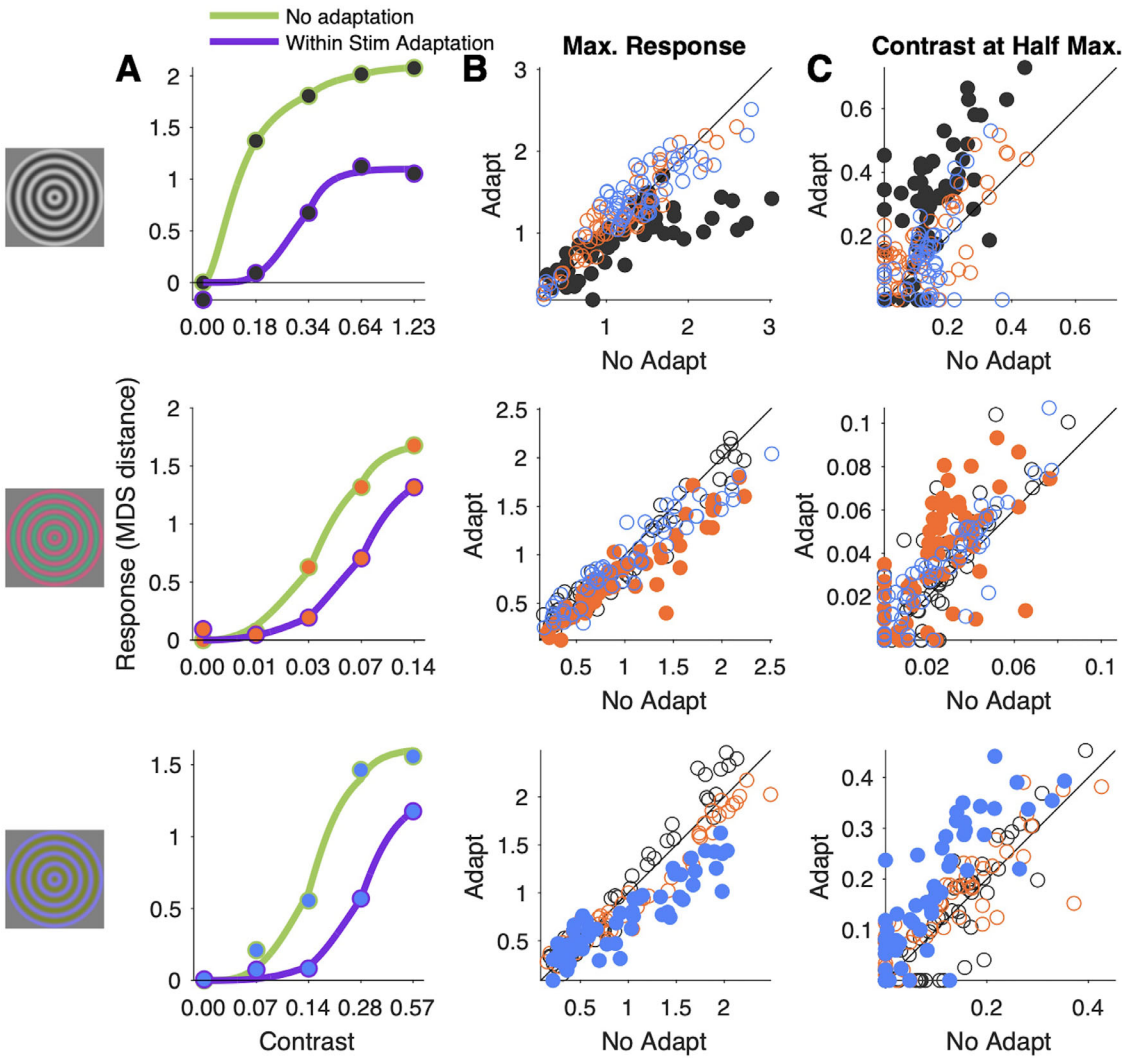

Figure 6. Effect of adaptation on the shape of the contrast response functions. Here we fit Naka-Rushton equations to the average (n = 6) MDS-based contrast response for each 10 ms time bin. (A) Example average contrast responses (*dots*) for within-stimulus adaptation, and Naka-Rushton fits (*lines*) for data from around the first peak (175–275 ms): see Supplementary Material for data across each 10 ms time bins (as movies). (B, C) The best fitting Naka-Rushton equations were summarized by two measures: their maximum response (B) and the contrast at which they reached half their maximum (C). These summary values are plotted with one marker for each time bin (every 10 ms from 50 ms to 600 ms), for no adapt versus adapt; the color of the marker indicates the adaptation condition, and *filled markers* highlight cases of within-stimulus adaptation.

adaptation was stronger than the cross-stimulus adaptation.

The effects of adaptation on the shape of the contrast response functions are shown in Figure 6 (equivalent figures with data from ventral and dorsal visual cortex are shown in the Supplementary Material). Single-neuron studies have shown that adaptation can lead to a multiplicative scaling down of responses (a response-gain effect) and also a rightward shift of the contrast-response curve to higher contrast (a contrast-gain effect) (Albrecht, Farrar, & Hamilton, 1984; Bonds, 1991; Sclar, Lennie, & DePriest, 1989). To test for both of these effects we described each contrast-response function in terms of its maximum response, as well as the contrast at which it reached half the maximum. The latter measure would not be influenced by a purely response-gain effect even in cases of strong adaptation. In each case of within-stimulus adaptation, we found that curves reached half-maximum at higher contrasts in the adapted conditions, ruling out purely response-gain changes. We also found stimulus-specific reductions in maximum response for all stimuli. This pattern of effects could result from adaptation inducing either pure contrast-gain or a combination of response- and contrast gain changes.

To facilitate comparison with the psychophysical measurements, we acquired previously (Goddard et al., 2019), we re-plot these in Figure 7, along with

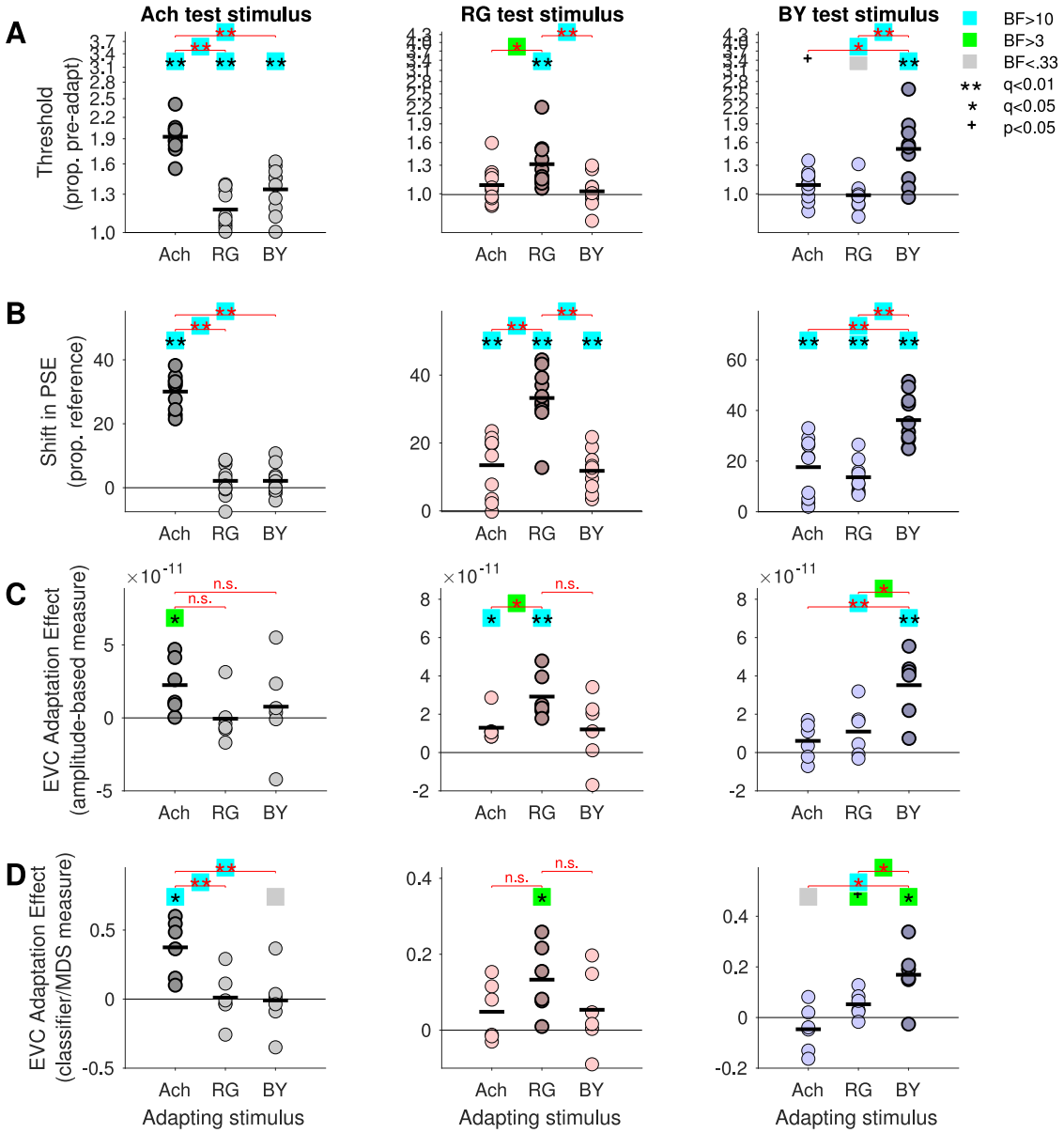

Figure 7. Comparison of adaptation effects across psychophysical and MEG measurements in EVC. (A, B) Changes in psychophysical detection thresholds (A) and points of subjectively equal contrast (B): data replotted from Goddard et al. (2019), Figure 7. (C, D) MEG adaptation effects based on differences between the area under the contrast response function of the test stimulus without adaptation and during adaptation, where the contrast response functions were measured using univariate (C) and classifier/MDS (D) metrics (MDS: responses were averaged across 50-600 ms to match epoch for amplitude-based analysis). In each plot, the circular markers show values for each participant (A, B: n = 10; C, D: n = 6), along with the mean (*thick black line*). *Black markers* above the data indicate cases of significant adaptation effects, whereas *red markers* indicate whether adaptation effects were greater in the within-stimulus compared to cross-stimulus conditions, in each case FDR corrected (** q < 0.01, * q < 0.05) or approaching significance (+ $p < 0.05$, not FDR corrected). Results with moderate (BF > 3) or strong effects (BF > 10), are highlighted with green or cyan squares respectively. Cases with at least moderate evidence in favor of a null effect (BF < 0.33) are indicated with a grey square. See Supplementary Table S1 for exact statistical values.

summaries of the adaptation effects measured with MEG using amplitude-based response differences (Figure 7C) and the responses differences across the average (50-600 ms, matching the epoch for amplitude-based analysis) of the MDS-based contrast response measures (Figure 7D). For each combination of adapting and test stimulus, we used a one-sided *t*-test to test whether the observed adaptation effect

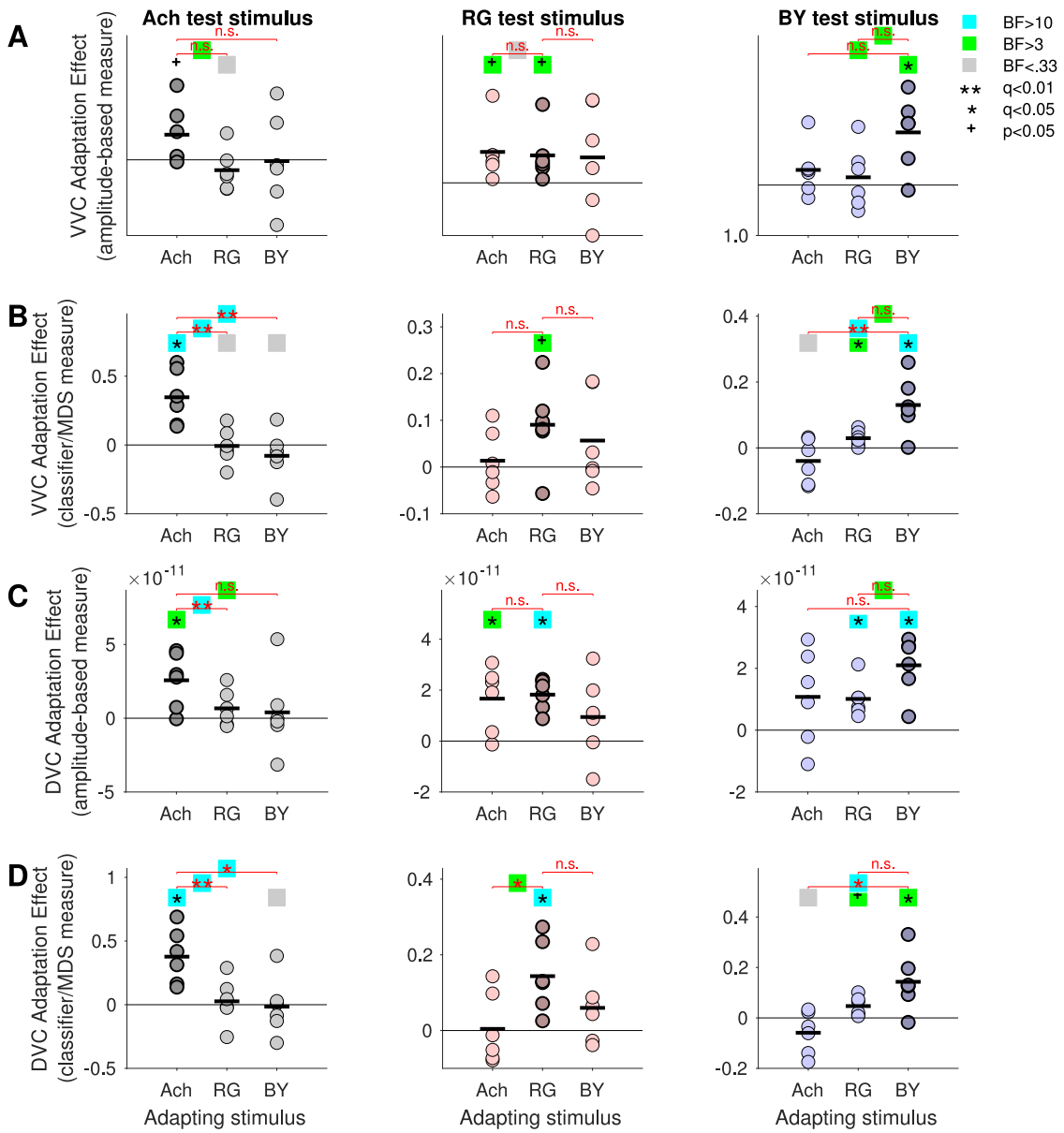

Figure 8. Comparison of adaptation effects using both MEG measurements in VVC (A, B) and DVC (C, D), measured using univariate (A, C) and classifier/MDS (B, D) metrics. Other plotting conventions are as in Figure 7.

was greater than zero. Across tests we applied a false discovery rate correction for multiple comparisons (Benjamini & Hochberg, 1995). For all stimuli there was significant within-stimulus adaptation (except for the BY stimulus using the MDS-metric, which was only marginally significant: $p < 0.05$, uncorrected for multiple comparisons). Across all stimuli and both analysis method the only case of cross-stimulus adaptation that was significant was the Ach adaptor on the RG test stimulus ($q < 0.05$).

Analyses equivalent to those in Figures 7C–D were also performed for data from the VVC and DVC regions of interest, and the results of these are shown in Figure 8. Full details of all statistical testing are given in the Supplementary Material.

Discussion

We used MEG to measure the effect of adaptation on contrast response for achromatic, isoluminant red-green (RG) and S-cone isolating (BY) stimuli. Previously, we found that, while behavioral adaptation effects for these stimuli were highly selective, BOLD adaptation showed strong cross-stimulus adaptation, with little evidence of selectivity (Goddard et al., 2019; Mullen et al., 2015). Here we found that MEG adaptation effects were dissimilar to the BOLD adaptation effects, with an absence of strong cross-stimulus adaptation, but showed good agreement with the selective psychophysical effects of contrast adaptation.

MEG contrast adaptation reflects perceptual effects

Overall, the effects of contrast adaptation on the MEG responses were in good agreement with the perceptual effects. MEG adaptation effects, like the behavioral effects, showed strong selectivity, with weak or absent cross-stimulus adaptation. This pattern of selectivity is also consistent with previous VEP results showing selectivity of chromatic contrast adaptation effects within the isoluminant plane (Duncan et al., 2012). Unlike in previous studies using VEPs to measure chromatic and achromatic contrast adaptation, here we included cross-adaptation conditions to measure interactions between achromatic and chromatic stimuli, and we measured the effects of adaptation on test stimuli of a range of contrasts.

In measuring responses across a range of stimulus contrasts, we found a pattern of within-stimulus adaptation. Although contrast-gain was evident for both chromatic and achromatic stimuli, there was some evidence suggesting that response gain played a larger role for the achromatic stimuli than for chromatic stimuli, with greater evidence of a reduction in the maximum response (Figure 6). However, this difference may not reflect a genuine difference in contrast adaptation effects, because responses to the (unadapted) achromatic test stimuli showed saturation at higher contrasts, whereas responses to the chromatic stimuli did not. Although our present data cannot distinguish between pure contrast gain and combined contrast and response gain for chromatic stimuli, future work using a different range of test contrasts may be able to differentiate between these.

The pattern of cross-stimulus adaptation effects on MEG contrast adaptation are in the direction of selectivity in each case, as in the behavioral effects of adaptation, although these differences did not reach statistical significance in all cases. In our previous psychophysical work (Figures 7A, 7B), we measured adaptation using two types of task, threshold detection and suprathreshold contrast matching, and we found that for both tasks within-stimulus adaptation was greater than cross-stimulus adaptation revealing selectivity for all stimulus combinations, consistent with previous literature (e.g., Krauskopf et al., 1982; Webster & Mollon, 1994). We also found some task-dependent differences. For detection thresholds, achromatic detection showed some cross-adaptation by the chromatic adaptors, which induced small but significant elevation of achromatic detection thresholds, whereas the achromatic adaptor did not affect detection of the chromatic stimuli. Conversely, for suprathreshold perceived contrast measurements, the chromatic test stimuli showed some cross adaptation by the achromatic adaptor as well as the other chromatic adaptor, with small but significant changes following adaptation, whereas achromatic perceived contrast was unaffected by the chromatic adaptors. It is not clear what the origins of these difference are and why achromatic detection shows less selectivity than achromatic perceived contrast.

Although the MEG data do not show clear evidence favoring either of these patterns of cross-stimulus adaptation effects, the two significant cross-stimulus adaptation effects (Ach adaptor on RG test and RG adaptor on BY test) are consistent with the pattern of effects for suprathreshold contrast judgements. Moreover, the fact that the contrast values for adaptor and test stimuli in MEG are all suprathreshold make it more likely that the MEG data would reflect the behavioral results for suprathreshold contrast perception than detection thresholds. Overall, our MEG adaptation results show selective effects that are broadly similar to the behavioral data.

An aim of our present study was to compare contrast adaptation effects across different visual cortical areas, which we divided into early (V1, V2, V3), ventral (hV4, VO1, VO2), and dorsal (LO, V3A/B, hMT+). Human fMRI studies show the high responsiveness of ventral areas to color (e.g., Brewer et al., 2005; Goddard et al., 2011; Lafer-Sousa, Conway, & Kanwisher, 2016; Mullen et al., 2007). Mullen et al. (2015) found evidence of selective adaptation to L/M isolating stimuli in ventral area VO of the ventral visual cortex, along with some selectivity for achromatic contrast in the dorsal cortical regions. Although MEG signals cannot be resolved with the spatial precision of fMRI, source reconstruction can be improved by including a forward model based on the participant's individual anatomy from an MRI image, as here, and previous studies have reported distinct effects in early and ventral visual areas (e.g., Bartsch et al., 2017). Despite this, we found very similar contrast adaptation effects across early, ventral and dorsal visual cortex (see Supplementary Material). This may reflect broadly similar contrast adaptation effects across visual cortex, but given the spatial uncertainty of MEG, we cannot rule out signal leakage between our regions of interest, which could have obscured any inter-regional differences.

A novel method for time-resolved measurement of contrast response functions

We have introduced a new tool for measuring how contrast response functions change over time, with fine temporal resolution. Methods such as MEG, electroencephalographic (EEG), and electrophysiological recordings allow millisecond resolution of neural activity, but traditional analysis methods often use metrics, such as response amplitude or response delay, that reduce data to a one or two

values per condition, as in the response amplitude analysis used here, where we obtained a single estimate of the contrast response function for each condition. More recently, classification-based analyses, applied within short time bins, have been applied to MEG and EEG recordings (e.g., Carlson, Hogendoorn, Kanai, Mesik, & Turret, 2011; Cichy, Pantazis, & Oliva, 2014; Goddard et al., 2016) and to multi-unit electrophysiological recordings (e.g., Goddard et al., 2017; Zavitz & Price, 2019), which is one method that allows the response dynamics to be explored, and to examine differences between conditions over time, from stimulus onset until the end of the trial. MDS has previously been applied to dissimilarity matrices as an exploratory method, to visualize the organizational principles present in the neural representation of the stimuli (e.g., Kriegeskorte, Mur, Ruff, Kiani, Bodurka, Esteky, Tanaka, & Bandettini, 2008).

However, here we are not applying MDS to discover an unknown response dimension but using it to reconstruct the relationship between a prespecified feature dimension (stimulus contrast) and response. We see the primary benefit of this approach as increasing signal to noise relative to other analyses. Comparing the response to each stimulus with the response to a blank screen using a difference (as in the response amplitude analysis) or with a classification analysis (equivalent to a single row of the dissimilarity matrix in Figure 4C) does not make use of the information captured by the pairwise classification analyses of each stimulus. Conversely, our MDS approach constructs the contrast response functions using information present across each pairwise comparison in the dissimilarity matrix. We found that this method yielded robust estimates (i.e., response functions that typically monotonically increased with contrast) even when based on data from single 10 ms time bin (see Figure 5, and videos in Supplementary Material). In our experiment we found that the effects of adaptation were remarkably consistent across the duration of the stimulus-induced response, but because it allows for the contrast response to be estimated within short time bins of data, this approach could yield useful insights into how the population contrast response changes over time in future MEG/EEG or multi-unit electrophysiological experiments.

Implications for understanding BOLD adaptation effects

The strong but unselective adaptation found in our previous BOLD adaptation experiments, especially for achromatic and S-cone isolating stimuli, was surprising given the psychophysical evidence for selective adaptation measured psychophysically under broadly similar conditions (Mullen et al., 2015; Goddard et al., 2019). Here, using MEG measurements, we found strong within-stimulus contrast adaptation was evident from the earliest part of the stimulus-induced response in all areas (see Figure 5). Cross-stimulus adaptation effects tended to be weaker, and within-stimulus adaptation significantly exceeded cross-stimulus adaptation in some, but not all cases. Overall, this suggests that the strong cross-stimulus BOLD adaptation effects observed previously do not reflect adaptation of the same mechanisms as captured by behavioral responses or MEG.

There were differences between the experimental design used in our previous fMRI work and in the current MEG study, but we think it unlikely that these differences account for the discrepancy in results. In particular, the temporal parameters of the fMRI designs were chosen to suit the slow temporal dynamics of the BOLD response: test stimuli had the same spatiotemporal contrast modulations but were grouped into 18-second blocks of a contrast discrimination task (rather than single trials, as in the psychophysical and MEG experiments). Additionally, in the fMRI design the no-adapt and adapt trials were interleaved within each experimental session, whereas in the psychophysical and MEG experiments all no-adapt trials were collected prior to any adaptation. These paradigm differences may have resulted in some differences in the adaptation effects measured across modalities, but they cannot account for the main discrepancy in the selectivity of adaptation. The paradigm differences could have reduced the overall level of contrast adaptation in the BOLD experiments, but the low level of selectivity observed in the fMRI experiments were not driven by low adaptation effects overall, but by surprisingly strong cross-stimulus adaptation, especially in the case of Ach/BY stimulus pairs.

In our previous work (Goddard et al., 2019), we discussed other instances where fMRI adaptation has failed to reveal selectivity when it might be expected (e.g. Boynton & Finney, 2003; Murray et al., 2006). We do not believe it likely that BOLD adaptation effects are partly driven by adaptation of the hemodynamic response, since work on the effects of adaptation on neurovascular-coupling suggest that BOLD measurements will tend to underestimate, rather than overestimate, neural adaptation effects (Larsson & Harrison, 2015; Moradi & Buxton, 2013). Instead, we speculated that the strong cross-adaptation effects might be driven by the fact that BOLD signals reflect the summed activity of large numbers of both excitatory and inhibitory neurons (both driver and modulator neurons) and includes non-spiking activity (Logothetis, 2008). Divisive normalization is considered widespread in cortical function (e.g., Heeger, 1992), and BOLD adaptation would reflect the effects of adaptation on driver and modulator spiking and

non-spiking activity, respectively, whereas spiking output and perception would correspond to the ratio or balance of these mechanisms. It is unclear how the spiking and non-spiking activity of driver and modulator neurons, and their ratio would be reflected in the MEG signals. Signals measured with MEG are believed to be driven primarily by magnetic induction arising from ionic currents, including post-synaptic potentials (Baillet, 2017). However, unlike the BOLD adaptation effects, the contrast adaptation effects measured with MEG show a similarly high degree of selectivity as the perceptual effects. This demonstrates that the divergence between BOLD adaptation effects and perceptual adaptation effects is at least partly specific to the signals captured in the BOLD signal.

Conclusions

We found that MEG measures of contrast adaptation were closely aligned with the highly selective perceptual effects of adaptation, unlike previously reported BOLD adaptation effects. We introduced a new method for measuring contrast response functions for each time sample in an MEG dataset, which could be applied in future work to explore how contrast response functions change over time after stimulus onset.

Keywords: MEG, fMRI, BOLD, visual cortex, multivariate pattern classification analysis (MVPA), multi-dimensional scaling (MDS), contrast adaptation

Acknowledgments

The authors thank Marc Lalancette for advice on MEG protocols. We thank all our participants for their assistance with data collection.

Funded by Canadian Institutes of Health Research (CIHR) grants 153277 and 10819 to KTM. EG was partly supported by an Australian Research Council DECRA fellowship (DE200100139).

Commercial relationships: none.
Corresponding author: Kathy T. Mullen.
Email: kathy.mullen@mcgill.ca.
Address: McGill Vision Research, Department of Ophthalmology & Visual Sciences, McGill University, Montreal, QC, H3G1A4, Canada.

References

Albrecht, D. G., Farrar, S. B., & Hamilton, D. B. (1984). Spatial contrast adaptation characteristics of neurones recorded in the cat's visual cortex. *The Journal of Physiology, 347*, 713–739.

Baillet, S. (2017). Magnetoencephalography for brain electrophysiology and imaging. *Nature Neuroscience, 20*(3), 327–339, https://doi.org/10.1038/nn.4504.

Bartsch, M. V., Loewe, K., Merkel, C., Heinze, H.-J., Schoenfeld, M. A., Tsotsos, J. K., . . . Hopf, J.-M. (2017). Attention to Color Sharpens Neural Population Tuning via Feedback Processing in the Human Visual Cortex Hierarchy. *Journal of Neuroscience, 37*(43), 10346–10357, https://doi.org/10.1523/JNEUROSCI.0666-17.2017.

Benjamini, Y., & Hochberg, Y. (1995). Controlling the False Discovery Rate: A Practical and Powerful Approach to Multiple Testing. *Journal of the Royal Statistical Society. Series B (Methodological), 57*(1), 289–300.

Blakemore, C., & Campbell, F. W. (1969). On the existence of neurones in the human visual system selectively sensitive to the orientation and size of retinal images. *Journal of Physiology, 203*(1), 237–260.

Blakemore, C., & Nachmias, J. (1971). The orientation specificity of two visual after-effects. *The Journal of Physiology, 213*(1), 157–174.

Bonds, A. B. (1991). Temporal dynamics of contrast gain in single cells of the cat striate cortex. *Visual Neuroscience, 6*(3), 239–255, https://doi.org/10.1017/s0952523800006258.

Boynton, G. M., & Finney, E. M. (2003). Orientation-specific adaptation in human visual cortex. *The Journal of Neuroscience: The Official Journal of the Society for Neuroscience, 23*(25), 8781–8787.

Bradley, A., Zhang, X., & Thibos, L. (1992). Failures of isoluminance caused by ocular chromatic aberrations. *Applied Optics, 31*(19), 3657–3667.

Brainard, D. H. (1997). The Psychophysics Toolbox. *Spatial Vision, 10*(4), 433–436.

Brewer, A. A., Liu, J., Wade, A. R., & Wandell, B. A. (2005). Visual field maps and stimulus selectivity in human ventral occipital cortex. *Nature Neuroscience, 8*(8), 1102–1109, https://doi.org/10.1038/nn1507.

Campbell, F. W., & Maffei, L. (1970). Electrophysiological evidence for the existence of orientation and size detectors in the human visual system. *The Journal of Physiology, 207*(3), 635–652, https://doi.org/10.1113/jphysiol.1970.sp009085.

Carlson, T. A., Hogendoorn, H., Kanai, R., Mesik, J., & Turret, J. (2011). High temporal resolution decoding of object position and category. *Journal of Vision, 11*(10), 9, 1–7, https://doi.org/10.1167/11.10.9.

Cichy, R. M., Pantazis, D., & Oliva, A. (2014). Resolving human object recognition in space and time. *Nature Neuroscience, 17*(3), 455–462, https://doi.org/10.1038/nn.3635.

Cottaris, N. P. (2003). Artifacts in spatiochromatic stimuli due to variations in preretinal absorption and axial chromatic aberration: Implications for color physiology. *Journal of the Optical Society of America A-Optics Image Science and Vision, 20*(9), 1694–1713.

Dale, A. M., Fischl, B., & Sereno, M. I. (1999). Cortical surface-based analysis. I: Segmentation and surface reconstruction. *Neuroimage, 9*(2), 179–194.

Dong, X., Du, X., & Bao, M. (2020). Repeated Contrast Adaptation Does Not Cause Habituation of the Adapter. *Frontiers in Human Neuroscience, 14*, 589634, https://doi.org/10.3389/fnhum.2020.589634.

Duncan, C. S., Roth, E. J., Mizokami, Y., McDermott, K. C., & Crognale, M. A. (2012). Contrast adaptation reveals increased organizational complexity of chromatic processing in the visual evoked potential. *Journal of the Optical Society of America. A, Optics, Image Science, and Vision, 29*(2), A152–156, https://doi.org/10.1364/JOSAA.29.00A152.

Engel, S. A. (2005). Adaptation of oriented and unoriented color-selective neurons in human visual areas. *Neuron, 45*(4), 613–623.

Engel, S. A., & Furmanski, C. S. (2001). Selective adaptation to color contrast in human primary visual cortex. *Journal of Neuroscience, 21*(11), 3949–3954.

Engel, S. A., Rumelhart, D. E., Wandell, B. A., Lee, A. T., Glover, G. H., Chichilnisky, E. J., . . . Shadlen, M. N. (1994). FMRI of human visual cortex. *Nature, 369*(6481), 525.

Fang, F., Murray, S. O., Kersten, D., & He, S. (2005). Orientation-tuned FMRI adaptation in human visual cortex. *Journal of Neurophysiology, 94*(6), 4188–4195.

Farnsworth, D. (1957). *The Farnsworth-Munsell 100-hue test for the examination of color discrimination.* Newburgh, NY: Macbeth, a division of Kollmorgen Corp.

Fischl, B., Sereno, M. I., & Dale, A. M. (1999). Cortical surface-based analysis. II: Inflation, flattening, and a surface-based coordinate system. *Neuroimage, 9*(2), 195–207.

Gardner, J. L., Sun, P., Waggoner, R. A., Ueno, K., Tanaka, K., & Cheng, K. (2005). Contrast adaptation and representation in human early visual cortex. *Neuron, 47*(4), 607–620.

Gibson, J. J., & Radner, M. (1937). Adaptation, after-effect and contrast in the perception of tilted lines. I. Quantitative studies. *Journal of Experimental Psychology, 20*(5), 453–467, https://doi.org/10.1037/h0059826.

Goddard, E., Carlson, T. A., Dermody, N., & Woolgar, A. (2016). Representational dynamics of object recognition: Feedforward and feedback information flows. *Neuroimage, 128*, 385–397, https://doi.org/10.1016/j.neuroimage.2016.01.006.

Goddard, E., Chang, D. H. F., Hess, R. F., & Mullen, K. T. (2019). Color contrast adaptation: FMRI fails to predict behavioral adaptation. *NeuroImage, 201*, 116032, https://doi.org/10.1016/j.neuroimage.2019.116032.

Goddard, E., Mannion, D. J., McDonald, J. S., Solomon, S. G., & Clifford, C. W. G. (2011). Color responsiveness argues against a dorsal component of human V4. *Journal of Vision, 11*(4), 3, 1–21, https://doi.org/10.1167/11.4.3.

Goddard, E., & Mullen, K. T. (2020). FMRI representational similarity analysis reveals graded preferences for chromatic and achromatic stimulus contrast across human visual cortex. *NeuroImage, 215*, 116780, https://doi.org/10.1016/j.neuroimage.2020.116780.

Goddard, E., Solomon, S. G., & Carlson, T. A. (2017). Dynamic Population Codes of Multiplexed Stimulus Features in Primate Area MT. *Journal of Neurophysiology, 118*(1), 203–218, https://doi.org/10.1152/jn.00954.2016.

Grill-Spector, K., & Malach, R. (2001). fMR-adaptation: A tool for studying the functional properties of human cortical neurons. *Acta Psychologica, 107*(1–3), 293–321, https://doi.org/10.1016/s0001-6918(01)00019-1.

Heeger, D. J. (1992). Normalization of cell responses in cat striate cortex. *Visual Neuroscience, 9*(2), 181–197.

Huang, M. X., Mosher, J. C., & Leahy, R. M. (1999). A sensor-weighted overlapping-sphere head model and exhaustive head model comparison for MEG. *Physics in Medicine and Biology, 44*, 423–440, https://doi.org/10.1088/0031-9155/44/2/010.

Huk, A., Dougherty, R., & Heeger, D. (2002). Retinotopy and functional subdivision of human areas MT and MST. *Journal of Neuroscience, 22*(16), 7195–7205.

Ishihara, S. (1990). *Ishihara's tests for color-blindness, 38 plate ed.* Tokyo: Kanehara, Shuppan Co. Ltd.

Kass, R. E., & Raftery, A. E. (1995). Bayes Factors. *Journal of the American Statistical Association, 90*(430), 773–795, https://doi.org/10.1080/01621459.1995.10476572.

Kleiner, M., Brainard, D., & Pelli, D. G. (2007). What's new in Psychtoolbox-3? *Perception, 36*, *ECVP Abstract Supplement*.

Kohn, A. (2007). Visual adaptation: Physiology, mechanisms, and functional benefits. *Journal of Neurophysiology, 97*(5), 3155–3164.

Krauskopf, J., Williams, D. R., & Heeley, D. W. (1982). Cardinal directions of color space. *Vision Research, 22*(9), 1123–1131.

Krauskopf, J., Williams, D. R., Mandler, M. B., & Brown, A. M. (1986). Higher order color mechanisms. *Vision Research, 26*(1), 23–32.

Krekelberg, B. (2021). *klabhub/bayesFactor: Ttest updates (v2.2.0)*. Geneva: Zenodo, https://doi.org/10.5281/zenodo.5707551.

Krekelberg, B., Boynton, G. M., & van Wezel, R. J. A. (2006). Adaptation: From single cells to BOLD signals. *Trends in Neurosciences, 29*(5), 250–256.

Kriegeskorte, N., Mur, M., Ruff, D. A., Kiani, R., Bodurka, J., Esteky, H., Tanaka, K., … Bandettini, P. A. (2008). Matching categorical object representations in inferior temporal cortex of man and monkey. *Neuron, 60*(6), 1126–1141, https://doi.org/10.1016/j.neuron.2008.10.043.

Lafer-Sousa, R., Conway, B. R., & Kanwisher, N. G. (2016). Color-Biased Regions of the Ventral Visual Pathway Lie between Face- and Place-Selective Regions in Humans, as in Macaques. *Journal of Neuroscience, 36*(5), 1682–1697, https://doi.org/10.1523/JNEUROSCI.3164-15.2016.

Larsson, J., & Harrison, S. J. (2015). Spatial specificity and inheritance of adaptation in human visual cortex. *Journal of Neurophysiology, 114*(2), 1211–1226, https://doi.org/10.1152/jn.00167.2015.

Larsson, J., & Heeger, D. J. (2006). Two retinotopic visual areas in human lateral occipital cortex. *Journal of Neuroscience, 26*(51), 13128–13142.

Logothetis, N. K. (2008). What we can do and what we cannot do with fMRI. *Nature, 453*(7197), 869–878.

Michna, M. L., Yoshizawa, T., & Mullen, K. T. (2007). S-cone contributions to linear and non-linear motion processing. *Vision Research, 47*(8), 1042–1054, https://doi.org/10.1016/j.visres.2007.01.014.

Moradi, F., & Buxton, R. B. (2013). Adaptation of cerebral oxygen metabolism and blood flow and modulation of neurovascular coupling with prolonged stimulation in human visual cortex. *NeuroImage, 82*, 182–189, https://doi.org/10.1016/j.neuroimage.2013.05.110.

Morey, R. D., & Wagenmakers, E.-J. (2014). Simple relation between Bayesian order-restricted and point-null hypothesis tests. *Statistics & Probability Letters, 92*, 121–124, https://doi.org/10.1016/j.spl.2014.05.010.

Movshon, J. A., & Lennie, P. (1979). Pattern-selective adaptation in visual cortical-neurons. *Nature, 278*(5707), 850–852.

Mullen, K. T. (1985). The contrast sensitivity of human colour vision to red-green and blue-yellow chromatic gratings. *Journal of Physiology, 359*, 381–400.

Mullen, K. T., Chang, D. H. F., & Hess, R. F. (2015). The selectivity of responses to red-green colour and achromatic contrast in the human visual cortex: An fMRI adaptation study. *The European Journal of Neuroscience, 42*, 2923–2933, https://doi.org/10.1111/ejn.13090.

Mullen, K. T., Dumoulin, S. O., & Hess, R. F. (2008). Color responses of the human lateral geniculate nucleus: Selective amplification of S-cone signals between the lateral geniculate nucleno and primary visual cortex measured with high-field fMRI. *European Journal of Neuroscience, 28*(9), 1911–1923.

Mullen, K. T., Dumoulin, S. O., McMahon, K. L., de Zubicaray, G. I., & Hess, R. F. (2007). Selectivity of human retinotopic visual cortex to S-cone-opponent, L/M-cone-opponent and achromatic stimulation. *European Journal of Neuroscience, 25*(2), 491–502, https://doi.org/10.1111/j.1460-9568.2007.05302.x.

Mullen, K. T., Thompson, B., & Hess, R. F. (2010). Responses of the human visual cortex and LGN to achromatic and chromatic temporal modulations: An fMRI study. *Journal of Vision, 10*, 13, https://doi.org/10.1167/10.13.13.

Murray, S. O., Olman, C. A., & Kersten, D. (2006). Spatially specific FMRI repetition effects in human visual cortex. *Journal of Neurophysiology, 95*(4), 2439–2445, https://doi.org/10.1152/jn.01236.2005.

Ohzawa, I., Sclar, G., & Freeman, R. D. (1982). Contrast gain control in the cat visual cortex. *Nature, 298*(5871), 266–268.

Pelli, D. G. (1997). The VideoToolbox software for visual psychophysics: Transforming numbers into movies. *Spatial Vision, 10*(4), 437–442.

Rabin, J., Switkes, E., Crognale, M., Schneck, M. E., & Adams, A. J. (1994). Visual evoked potentials in three-dimensional color space: Correlates of spatio-chromatic processing. *Vision Research, 34*(20), 2657–2671.

Rosenthal, I. A., Singh, S. R., Hermann, K. L., Pantazis, D., & Conway, B. R. (2021). Color Space Geometry Uncovered with Magnetoencephalography. *Current Biology: CB, 31*(3), 515–526.e5, https://doi.org/10.1016/j.cub.2020.10.062.

Sankeralli, M. J., & Mullen, K. T. (1996). Estimation of the L-, M-, and S-cone weights of the postreceptoral detection mechanisms. *JOSA A, 13*(5), 906–915.

Schira, M. M., Tyler, C. W., Breakspear, M., & Spehar, B. (2009). The foveal confluence in human visual cortex. *Journal of Neuroscience, 29*(28), 9050–9058.

Sclar, G., Lennie, P., & DePriest, D. D. (1989). Contrast adaptation in striate cortex of macaque. *Vision Research, 29*(7), 747–755.

Sereno, M. I., Dale, A. M., Reppas, J. B., Kwong, K. K., Belliveau, J. W., Brady, T. J., Rosen, B. R., . . . Tootell, R. B. (1995). Borders of multiple visual areas in humans revealed by functional magnetic resonance imaging. *Science, 268*(5212), 889–893.

Solomon, S. G., & Kohn, A. (2014). Moving sensory adaptation beyond suppressive effects in single neurons. *Current Biology, 24*(20), R1012–R1022, https://doi.org/10.1016/j.cub.2014.09.001.

Tadel, F., Baillet, S., Mosher, J. C., Pantazis, D., & Leahy, R. M. (2011). Brainstorm: A user-friendly application for MEG/EEG analysis. *Computational Intelligence and Neuroscience, 2011*, 879716, https://doi.org/10.1155/2011/879716.

Teichmann, L., Grootswagers, T., Carlson, T., & Rich, A. N. (2019). Seeing versus knowing: The temporal dynamics of real and implied colour processing in the human brain. *NeuroImage, 200*(15), 373–381, https://doi.org/10.1016/j.neuroimage.2019.06.062.

Teichmann, L., Quek, G. L., Robinson, A. K., Grootswagers, T., Carlson, T. A., & Rich, A. N. (2020). The Influence of Object-Color Knowledge on Emerging Object Representations in the Brain. *The Journal of Neuroscience: The Official Journal of the Society for Neuroscience, 40*(35), 6779–6789, https://doi.org/10.1523/JNEUROSCI.0158-20.2020.

Uusitalo, M. A., & Ilmoniemi, R. J. (1997). Signal-space projection method for separating MEG or EEG into components. *Medical & Biological Engineering & Computing, 35*(2), 135–140, https://doi.org/10.1007/BF02534144.

Webster, M. A. (2011). Adaptation and visual coding. *Journal of Vision, 11*(5), https://doi.org/10.1167/11.5.3.

Webster, M. A. (2015). Visual Adaptation. *Annual Review of Vision Science, 11*, 547–567.

Webster, M. A., & Mollon, J. D. (1994). The influence of contrast adaptation on color appearance. *Vision Research, 34*(15), 1993–2020.

Zavitz, E., & Price, N. S. C. (2019). Weighting neurons by selectivity produces near-optimal population codes. *Journal of Neurophysiology, 121*(5), 1924–1937, https://doi.org/10.1152/jn.00504.2018.